

The Adsorbate Electron Affinity Dependence of Femtosecond Electron Dynamics at Dielectric/Metal Interfaces

Kelly J. Gaffney, Simon H. Liu, Andre D. Miller, Paul Szymanski and Charles B. Harris*

*Department of Chemistry, University of California, Berkeley, California 94720, and
Chemical Sciences Division, E.O. Lawrence Berkeley National Laboratory, Berkeley, California 94720, U.S.A.*

The two photon photoemission technique has been utilized to investigate the adsorbate electron affinity dependence of interfacial electron transfer dynamics. The comparison of calculated and experimental results highlight a brief discussion of a dielectric continuum model. For the n-heptane/Ag(111) and the benzene/Ag(111) interfaces, the model effectively reproduces experimental image potential state properties. The model fails to adequately describe the influence of anthracene adsorbates on image potential state lifetimes, as demonstrated by the experimental and theoretical results. The experimental $n = 1$ lifetime of 1200 femtoseconds and binding energy of -0.53 eV for the anthracene bilayer differ greatly from the calculated values of 40 femtoseconds and -1.4 eV.

The application of femtosecond (fs) laser technology to two photon photoemission (TPPE) has transformed the experimental investigation of electron dynamics in metals and at metal surfaces. Indirect information has long been accessible via linewidth analysis of static spectra obtained from inverse photoemission,¹ and high resolution electron energy loss spectroscopy studies,² but the difficulty in distinguishing between phase and energy relaxation, as well as the complicating influence of inhomogeneous broadening, stresses the importance of directly measuring electron dynamics.

The two photon photoemission technique populates unoccupied electronic states with a pump pulse and photoemits the excited state electrons with a probe pulse, as depicted in Fig. 1(a). The binding energy of the unoccupied electronic states can be determined by measuring the kinetic energy of the photoemitted electrons and then subtracting the energy of the probe pulse photon. The excited state lifetimes can be determined by measuring the number of electrons detected as a function of time delay between the arrival of the pump and the probe pulses at the sample. The direct observation of excited state lifetimes constitutes the most significant advantage of TPPE (see Fig. 1).

Time resolved TPPE has been utilized to study many aspects of electron dynamics in metals and at metal surfaces. Numerous experimental investigations of hot electron dynamics have been conducted to date in an attempt to determine the influence of the metal band structure on electron dynamics.³⁻⁷ The phase resolved interferometric two photon photoemission studies of Petek and coworkers have directly determined the energy dependence of both population and phase decay for noble metal surfaces.³ As expected from Fermi liquid theory, electrons with energies near the Fermi level have the longest

lifetimes. The scattering times of electrons with energies far from the Fermi energy resemble those of the Drude model.^{3,5} The presence of occupied d-bands, however, results in significant deviations from Fermi liquid theory behavior. Initial studies of the spin dependence of hot electron lifetimes in ferromagnetic materials have also been conducted.^{6,8}

The energy and lifetime of the adsorbate electron affinity (EA) levels have received significant attention due to their proposed importance in metal surface photochemistry and

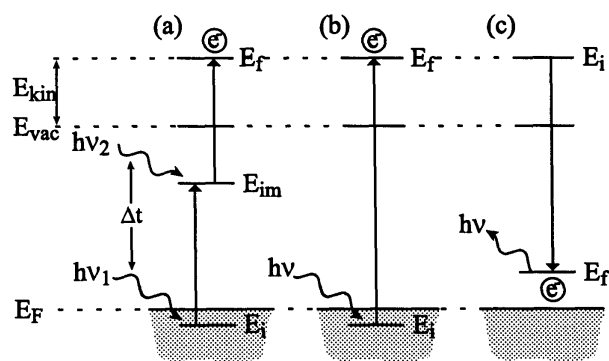


Fig. 1. (a) TPPE as described in the text. By varying the time delay between the pulses, Δt , the dynamics of excited states can be directly observed. (b) Photoemission uses one photon to probe occupied states below the Fermi energy. This technique is unable to access bound excited states, or directly observe electron dynamics. (c) Inverse photoemission scatters a monoenergetic beam of electrons from a surface and monitors the emitted light. This technique can access excited states, but with poor energy resolution and without direct time resolution.

charge injection at device interfaces.^{9,10} Understanding the role of hot electrons in electron induced dissociation has directed numerous studies of atoms and molecules chemically adsorbed on metal surfaces. The model system of CO adsorption on Cu has received the most extensive investigation.¹¹⁻¹³ Wolf and coworkers measured the lifetime of the $2\pi^*$ EA level to be 0.8-5 fs¹¹ and have determined the relative importance of direct and indirect excitation mechanisms for the population of unoccupied states at metal surfaces with substrate electrons.¹² Studies of the unoccupied anti-bonding orbital that results from Cs chemisorption on Cu have also been conducted.^{14,15} Ogawa et al. determined the lifetime of the unoccupied anti-bonding state of the Cs/Cu(111) system to be 50 fs,¹⁴ significantly longer than theory predicted.

Image potential states have also been observed for a wide class of metal/adsorbate interfaces. Image potential states result from the interaction between an electron outside of a surface and the surface polarization induced by the electron. The effect of the surface polarization can be represented as a positive image charge with a distance from the surface equal in magnitude, but opposite in direction, from that of the electron.^{16,17} The resultant Coulomb potential outside of a metal surface, $V(z) = -1/4z$, supports an infinite series of hydrogenic states that converge to the vacuum energy, i.e., image potential states. The proximity of image potential states to the surface (the expectation value of $n = 1$ lies roughly 3 Å outside the metal surface) makes image potential states highly sensitive to adsorbate induced variations in the interfacial electronic properties.

The influence of physically adsorbed atoms and molecules on interfacial electron dynamics has been demonstrated for a variety of adsorbates and substrates.^{13,16-19} The present manuscript will first describe the important influence of the adsorbate EA on image potential state lifetimes and binding energies. A dielectric continuum model that effectively reproduces the experimental findings for n-heptane and benzene adsorbates on the Ag(111) surface will be described. The paper will conclude with a presentation of the experimental and theoretical image potential state lifetimes and binding energies for the naphthalene/Ag(111) and anthracene/Ag(111) interfaces. The deviation between experiment and theory for anthracene demonstrates a significant limitation of the dielectric continuum model. An alternative model based upon the two band nearly free electron model has been constructed that effectively reproduces the experimental findings for both naphthalene and anthracene.²⁰

The differences in lifetimes and binding energies for the n-heptane/Ag(111) and the benzene/Ag(111) interfaces have been successfully explained through the use of a dielectric continuum model. Within this model, the most important dif-

ference between these two adsorbates is that benzene has an attractive EA, while n-heptane has a repulsive EA. The repulsive EA of the n-heptane layer effectively decouples the image potential states from the substrate, resulting in longer lifetimes and reduced binding energies.²¹ The attractive EA of the benzene layer produces image potential states that reside predominantly in the screened image potential at the benzene/Ag(111) interface, resulting in lifetimes and binding energies only weakly perturbed from the Ag(111) values.²² The experimental results for n-heptane and benzene demonstrate the significant variation in image potential state properties that result from variations in adsorbate EA. The $n = 1$ image potential state lifetimes and binding energies change from 36 fs and -0.77 eV for the bare Ag(111) to 1600 fs and -0.53 eV for a bilayer of n-heptane and 45 fs and -0.68 eV for a bilayer of benzene.

Dielectric continuum model calculations treat the adsorbate as a uniform dielectric layer.^{23,24} The potential outside of the substrate is modified by the EA, dielectric constant and width of the dielectric layer (see Fig. 2). Within the layer, the image potential is screened by the dielectric and converges to the EA level, $V(z) \approx -1/4\epsilon z - EA$, where ϵ represents the dielectric constant. Outside of the layer, the dielectric screens the interaction between the metal and the electron. Additionally, the electron is attracted to the polarization it induces in the overlayer, forming a second image potential. The total potential outside the layer is a sum of these two effects. To avoid singularities, the potential is cut off at the Fermi energy at the metal/adsorbate interface, and interpolated linearly at the adsorbate/vacuum interface.

The total potential outside of the substrate is used in a numerical integration of the Schrödinger equation. Eigenstates occur for binding energies where the wavefunction outside the surface matches the metal wavefunction at $z = 0$ and disappears as z goes to infinity. The metal wavefunction is represented by a two band nearly free electron model, using bulk silver parameters for the [111] direction. Fig. 2 depicts the calculated potentials and wavefunctions for a bilayer of benzene and a bilayer of n-heptane. The image potential state electrons described by these wavefunctions are expected to decay via a scattering process with the metal. This scattering process is enhanced for electronic wavefunctions that have a large overlap with the metal, resulting in shorter lifetimes.²⁵ Quantitative values for image potential electronic lifetimes can be obtained by determining the electron density of the calculated wavefunctions in the metal. Fig. 3 shows binding energies and lifetimes for molecules with several different EA, comparing the experimental results to calculated values.

In Fig. 2(a) the effect of adsorbed n-heptane, with a repulsive EA, can be observed. The potential in the n-heptane

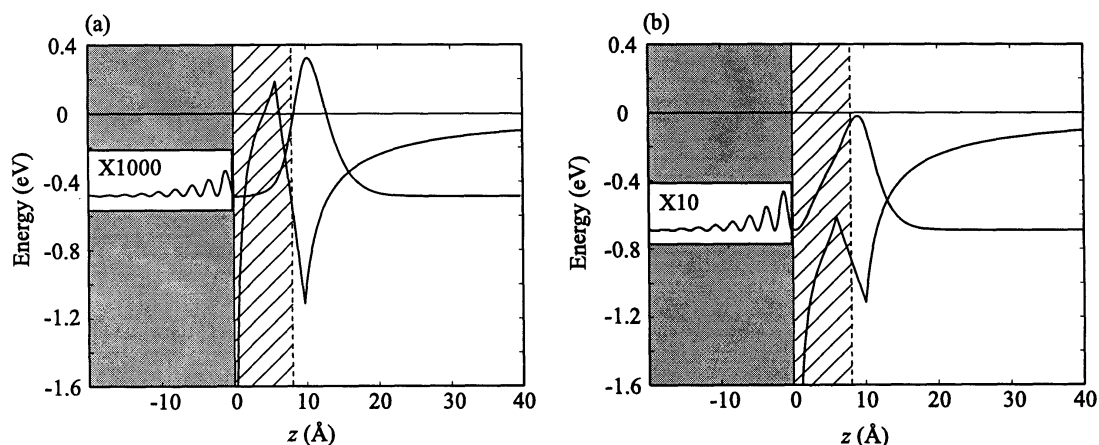


Fig. 2. Dielectric continuum model potentials and squared wavefunctions are plotted as a function of distance from the surface, z . The dashed vertical line corresponds to the layer/vacuum boundary. (a) An n-heptane overlayer with a repulsive EA results in a potential barrier, pushing the electron out to the layer/vacuum interface and decreasing the overlap with the metal. (b) A benzene overlayer with an attractive EA results in a larger overlap with both the benzene layer and the metal. Note the wavefunction amplitudes in the metal, which are inversely proportional to the electronic lifetimes. The wavefunction amplitudes in the metal are different by roughly two orders of magnitude, consistent with the large differences in experimental lifetimes.

layer converges to a value greater than the vacuum energy. The resultant barrier forces the image potential state electron to reside at the n-heptane/vacuum interface. The barrier effectively decouples the electron from the metal and significantly increases the image state lifetime. The effect of an adsorbed benzene layer, with an attractive affinity level, is shown in Fig. 2(b). The potential for the benzene layer converges to the

EA level, 0.6 eV below the vacuum energy. This results in an $n = 1$ image state positioned within the layer. The weak multilayer dependence of the calculated wavefunctions leads to multilayer independent $n = 1$ lifetimes, consistent with experimental findings.

The EA dependence of the $n = 1$ image potential state lifetimes and binding energies appear in Fig. 3. The signifi-

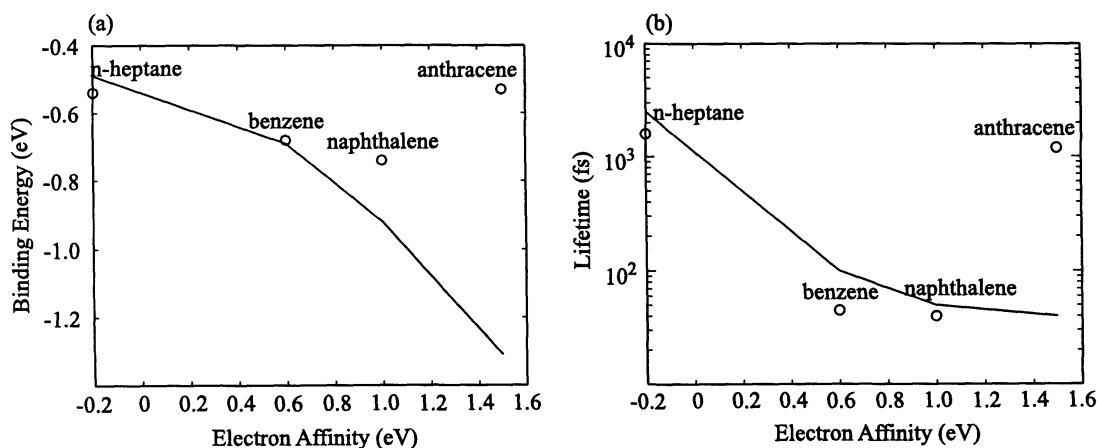


Fig. 3. Experimental (O) and calculated (—) values for (a) the binding energies and (b) the lifetimes of $n = 1$ image potential states as a function of EA . These values correspond to bilayer coverages. The calculations use typical values for layer thickness and dielectric constant, with the EA as the only varied parameter. This demonstrates the significant influence of the EA in the dielectric continuum model, but does not necessarily obtain the best agreement with experimental results. By choosing material specific parameters, excellent agreement has been achieved for benzene and n-heptane.^{21,22} The dielectric continuum model does not reproduce experimental values for anthracene when appropriate parameters are chosen.

cant deviation between the values predicted by the dielectric continuum model and those measured with TPPE for anthracene clearly demonstrate a significant weakness in the model. An alternative model based upon the two band nearly free electron model has been constructed that effectively reproduces the experimental findings for both naphthalene and anthracene.²⁰ This alternative model demonstrates that the coupling between the image potential and the adsorbate *EA* dictates the binding energies and lifetimes of the electronic states observed with TPPE. The energetic position of the adsorbate *EA* with respect to the energy of the image potential states at the adsorbate/vacuum boundary determines the strength of their interaction. The binding energies of *n* = 1 image potential states at metal surfaces vary from roughly -0.85 eV to -0.5 eV,²⁶ similar to the affinity level binding energy of benzene, -0.6 eV,²² and naphthalene, -1.0 eV,^{27,28} but significantly different than those of n-heptane, 0.2 eV,²⁹ and anthracene, -1.5 eV.^{28,30} The *EA* of benzene and naphthalene interact strongly with the *n* = 1 image potential state due to the small energy separation, while the *EA* of n-heptane and anthracene interact weakly due to the large energy separation. The experimental results presented in Fig. 3(b) clearly demonstrate this distinction.

The dielectric continuum model adequately explains image potential state properties for a variety of adsorbate materials, including saturated hydrocarbons, noble gases, and benzene. The inability of the model to reproduce the experimental lifetimes for anthracene clearly show a significant limitation in the dielectric continuum model. These results demonstrate the importance of femtosecond time resolution in the direct observation of electron dynamics at metal surfaces.

ACKNOWLEDGMENTS

This work was supported by the Director, Office of Energy Research, Office of Basic Energy Sciences, Chemical Sciences Division of the U.S. Department of Energy, under Contract No. DE-AC03-76SF00098. The authors acknowledge NSF support for specialized equipment used in the experiments described herein.

Received February 8, 2000.

Key Words

Adsorbate electron affinity; Interfacial electronic structure; Femtosecond two photon photoemission; Dielectric/metal interfaces.

REFERENCES

1. Smith, N. V.; Woodruff, D. P. *Prog. Surf. Sci.* **1986**, *21*, 295.
2. Avouris, Ph.; Persson, B. N. J. *J. Phys. Chem.* **1984**, *88*, 837.
3. Petek, H.; Ogawa, S. *Prog. Surf. Sci.* **1997**, *56*, 239.
4. Ogawa, S.; Nagano, H.; Petek, H. *Phys. Rev. B* **1997**, *55*, 10869.
5. Knoesel, E.; Hotzel, A.; Wolf, M. *Phys. Rev. B* **1998**, *57*, 12812.
6. Aeschlimann, M.; Bauer, M.; Pawlik, S. *Phys. Rev. Lett.* **1997**, *79*, 5158.
7. Campillo, I.; Pitarke, J. M.; Rubio, A.; Zarate, E.; Echenique, P. M. *Phys. Rev. Lett.* **1999**, *83*, 2230.
8. Scholl, A.; Baumgarten, L.; Jacquemin, R.; Eberhardt, W. *Phys. Rev. Lett.* **1997**, *79*, 5146.
9. Ho, W. *J. Phys. Chem.* **1996**, *100*, 13050.
10. Friend, R. H. et al. *Nature* **1999**, *397*, 121.
11. Bartels, L. et al. *Phys. Rev. Lett.* **1998**, *80*, 2004.
12. Wolf, M.; Hotzel, A.; Knoesel, E.; Velic, D. *Phys. Rev. B* **1999**, *59*, 5926.
13. Reuss, Ch. et al. *Phys. Rev. Lett.* **1999**, *82*, 153.
14. Ogawa, S.; Nagano, H.; Petek, H. *Phys. Rev. Lett.* **1999**, *82*, 1931.
15. Bauer, M.; Pawlik, S.; Aeschlimann, M. *Phys. Rev. B* **1999**, *60*, 5016.
16. Wong, C. M. et al. *J. Phys. Chem. B* **1999**, *103*, 282.
17. Ge, N.-H.; Wong, C. M.; Harris, C. B. *Acc. Chem. Res.* in press.
18. Hotzel, A.; Ishioka, K.; Knoesel, E.; Wolf, M.; Ertl, G. *Chem. Phys. Lett.* **1998**, *285*, 271.
19. Velic, D.; Hotzel, A.; Wolf, M.; Ertl, G. *J. Chem. Phys.* **1998**, *109*, 9155.
20. Gaffney, K. J.; Miller, A. D.; Liu, S. H.; Harris, C. B. to be published.
21. Lingle, Jr., R. L.; Ge, N.-H.; Jordan, R. E.; McNeill, J. D.; Harris, C. B. *Chem. Phys.* **1996**, *205*, 191.
22. Gaffney, K. J.; Wong, C. M.; Liu, S. H.; Miller, A. D.; McNeill, J. D.; Harris, C. B. *Chem. Phys.* **2000**, *251*, 99.
23. McNeill, J. D.; Lingle, Jr., R. L.; Jordan, R. E.; Padowitz, D. F.; Harris, C. B. *J. Chem. Phys.* **1997**, *48*, 711.
24. Hotzel, A.; Moos, G.; Ishioka, K.; Wolf, M.; Ertl, G. *App. Phys. B* **1999**, *68*, 615.
25. de Andres, P. L.; Echenique, P. M.; Flores, F. *Phys. Rev. B* **1989**, *39*, 10356.
26. Fauster, Th.; Steinmann, W. in *Electromagnetic Waves: Recent Developments in Research, Vol. 2. Photonic Probes of Surfaces*; Halevi, P., Ed.; Elsevier: Amsterdam,

- 1995; pp. 1-34.
27. Burrow, P. D.; Michejda, J. A.; Jordan, K. D. *J. Chem. Phys.* **1987**, 86, 9.
28. Silinsh, E. A.; Capek, V. *Organic Molecular Crystals: Interactions, Localization, and Transport Phenomena*; American Institute of Physics: New York, **1994**.
29. Allen, A. O. *U.S. Dept. of Commerce, NBS Report No. NSRDS-NBS 1976*, 58.
30. Schiedt, J.; Weinkauff, R. *Chem. Phys. Lett.* **1997**, 266, 201.